KAERI/TR-905/97

하나로 저유속 임계열유속 상관식 개발

(Development of Low Flow CHF Correlation for HANARO)

한 국 원 자 력 연 구 소

Korea Atomic Energy Research Institute

제 출 문

한국원자력연구소장 귀하

본 보고서를 기술보고서로 제출합니다.

제목 : 하나로 저유속 임계열유속 상관식 개발

(Development of Low Flow CHF Correlation for HANARO)

1997년 8월 일

주저자 : 박 철

공동저자 : 채희택

한기양

감수위원 : 김헌일

요 약

하나로의 자연대류 냉각 운전시 및 사고시 저유속 조건에서의 안전성 평가를 위한 임계열유속 상관식이 개발되었다. 임계열유속 조건에서 핀이 있는 가열봉에 대해 둘레를 따른 온도 및 열유속 분포를 계산하기 위하여 해석적 모델을 사용하였으며, 모델에 의해 예측된 가열표면 온도와 측정된 온도는 잘 맞는 것으로 나타났다. 핀이 달린 가열봉에서의 여러 가지 변수가 임계열유속에 미치는 영향은 일반적으로 핀이 없는 경우에 대해 알려진 경향과 일치하였다. 그리고, 핀에 의한 열전달 면적의 차이로 인해 임계 출력은 증가하나 임계열유속은 차이가 없는 것으로 나타나 국부적으로 핀은 임계열유속에 영향을 미치지 않는 것으로 판단된다. 기존의 핀이 없는 경우에 대한 임계열유속 상관식들은 핀이 있는 경우의 예측에서 큰 오차가 있는 것으로 나타나, 이를 보정한 새로운 상관식을 제시하였다. 새 상관식은 실험자료를 13.7%의 RMS 오차를 가지고 잘 예측한다. 상관식의 적용 범위는 아래와 같다.

- Pressure(kPa) 110 ~ 509
- Mass Flux($kg/m^2/s$) 26 ~ 404
- Inlet Subcooling(kJ/kg) 176 ~ 500
- Heat Flux (kW/m^2) 258 ~ 1415
- Hydraulic Dia.(mm) 7.3 ~ 13.66
- Critical Quality -0.034 ~ 0.702

Development of Low Flow CHF Correlation for HANARO

Cheol Park, Hee-Taek Chae, Gee-Yang Han

Abstract

A low flow CHF Correlation was developed for the safe operation of HANARO during the natural circulation cooling and the assessment of safety during the low flow condition of accident. The analytical model was applied to estimate the heat flux and the temperature distributions along the periphery of the fin at CHF conditions, and the predicted wall temperature at the sheath between the fins by the model agreed well with the measured one. The parametric trends of the CHF data for the finned geometry agreed with the general understanding from the previous studies for the unfinned annulus or tube geometries. It is revealed that the fin does not affect the CHF for low flow condition, although it increases the critical power due to larger heat transfer area. As the existing CHF correlation for unfinned geometry gave large deviation in predicting the experimental CHF data, a new correlation is proposed to predict the CHF for both finned and unfinned geometries at low flow and low pressure conditions. The developed correlation predicts the experimental CHF data with RMS error of 13.7%

The applicable range of CHF correlation is as follows,

Pressure(kPa)	110～509
Mass Flux(kg/m^2/s)	26～404
Inlet Subcooling(kJ/kg)	176～500
Heat Flux (kW/m^2)	258～1415
Hydraulic Dia.(mm)	7.3～13.66
Critical Quality	-0.034～0.702

Table of Contents

List of Tables

List of Figures

1. Introduction

The critical heat flux(CHF) condition is characterized by a sharp reduction in the local heat transfer coefficient due to the change of heat flux or cooling condition on the heater surface. The occurrence of this phenomenon in the reactor fuel leads to a sudden temperature increase of cladding, which results in rupture or melting of fuel. Hence, the CHF is considered to be one of the most important parameters in the design and safety analysis of a nuclear reactor. However, it is not always easy to accurately predict the onset of CHF owing to the extreme complexity of the heat and mass transfer processes responsible for the occurrence of CHF, and also because of the incomplete knowledge of the mechanisms involved, particularly, at low flow and low pressure conditions. Moreover, CHF is a function of geometry.

Research reactors generally require efficient heat removal from the fuel surface because they are designed to have high power density for obtaining high neutron flux. HANARO(High Flux Advanced Neutron Application Reactor)[KAERI,1996] adopted a finned fuel element to enhance heat transfer. However, the heat transfer characteristics including CHF for the finned fuel are quite different from those for the bare rods without fins used in power reactors, since the heat flux and the wall temperature vary considerably along the periphery of fins.

Review of previous works on the CHF for finned geometry described in next section indicates that the fin seems to positively affect on the enhancement of power load and CHF but the degrees may depend on the flow condition and the fin configuration, etc. However, little work has been done for the CHF in vertical annulus with the finned geometry at the low flow conditions. In particular, the effect of fin on CHF under low flow

condition has not been addressed. The existing CHF correlations for an annulus with unfinned heaters are also not applicable to the finned geometry, as will be shown later.

Thus, the objectives of the present work are to investigate the CHF characteristics for finned geometry, including fin effect on CHF, and to develop a CHF correlation for both finned and unfinned geometries under low flow and low pressure conditions. In this report, experiment and analysis of CHF for both unfinned and finned geometries are presented. The parametric trends of the test data are also discussed. The comparisons of existing correlations with the experimental data are done, and a new correlation is proposed to predict the CHF for both finned and unfinned geometries under low pressure and low flow conditions.

2. Previous Works on the CHF in a Finned Geometry

Mayer et al.(1988) carried out CHF experiments for a finned tube in a horizontal channel with a external cross flow range of 0.12 ~ 1.2 m/s. Their findings are: The maximum thermal load for finned tube was much higher than that for the plain tube, and the ratio of the maximum thermal loads for the finned tube and the plain tube decreases at the high degrees of subcooling and the high coolant velocities. The higher thermal load ratio at low flow is mainly due to the bubble nucleation along the overall periphery including fin tips. This means that the heat flux distribution at low flow is less steep than that at higher coolant velocity.

Kowalski et al.(1989) developed an one-dimensional analytical model to describe the surface heat flux distribution for the finned fuel element

simulator. This model was verified against two dimensional code MARC predictions and experimental data for single phase forced convection conditions in a velocity range of 0.7 ~ 7.0 m/s. The comparison of the fin heat flux by analytical model with MARC predictions showed good agreements. The one-dimensional assumption is generally justified since the temperature gradients normal to the direction of the major heat flow are small in metal material.

Shim et al.(1990) presented the results of test and analysis on the CHF for finned and unfinned geometry for subcooled flow boiling with high velocity larger than 1 m/s. They observed that the dry patch on the unfinned surface propagated circumferentially prior to the rupture while it on the finned surface was localized between fins at CHF condition. The peripheral heat flux distribution at CHF along the finned surface was calculated by the analytical model of Kowalski et al.[1989] and two dimensional numerical analysis, respectively. CHF values by analytical model agreed with the numerical solution within $\pm 6\%$. The reason was caused by an assumption of constant two phase boundary condition over the convective boundary although the fin side was on the single phase convection condition due to high subcooling. Another major finding from this study was that the presence of fins increased the CHF.

Experimental and analytical studies on the subcooled CHF for the finned heater in a vertical annulus were performed by Kowalski et al.(1994). The local heat flux was determined by a two dimensional finite element heat transfer model and convective heat transfer correlations. A correlation containing correction terms to represent the effect of the fin geometry was proposed and it showed 22% of standard deviation error. The applicable range of correlation for the mass flux was 390 ~ 8405 kg/m2/s. Correlation gives larger CHF value for finned geometry than that

for geometry without fins. They reported CHF first appeared on the fin root surface due to higher heat flux than that at fin side.

Grimly et al.(1988) conducted the CHF experiments with a fluorocarbon liquid film of 1 m/s velocity falling over a vertical heated surface with micro fins for electronic cooling. The result showed that the microfin surface enhanced nucleate boiling and CHF relative to a plain surface.

CHF experiments with internally finned tube were performed in a very high flow region with velocities larger than 5 m/s for the neutral beam injector by Araki et al.(1989). The measured heat load for an internally and externally finned tube was found to be larger than that for a smooth tube.

Collier(1972) quoted the use of fins as one of the methods to improve CHF.

3. Experimental Data

A total of 147 CHF data were obtained for a vertical annulus with both finned and unfinned heaters at the low flow and low pressure conditions. Test section geometries are given in table 1 together with each corresponding number of data. Two different quartz tubes were used to investigate the effect of the hydraulic diameter on critical heat flux. To determine the fin effect on CHF, the CHF test was conducted for both finned and unfinned geometries. For comparing the compatibility with AECL test data, the experiment with the same dimension of heaters and hydraulic diameter channels was also done(See Fig. 8). The ranges of test conditions and the estimated uncertainties are summarized in the table 2.

Details of experiment such as apparatus and test procedures can be found in Park et al.(1997).

4. Estimation of Local CHF

For the finned geometry, the heat flux and the temperature distributions are not uniform and vary considerably along the periphery of the fin. They are expected to be higher at the sheath halfway between fins. Hence, it is necessary to estimate the distributions of heat flux and temperature for the analysis of local phenomena such as CHF. In this study, the analytical model developed by Kowalski et al.(1989) is applied to determine local maximum CHF value.

The model assumed the following.

- The heat flux on the heater surface(oxide layer) is constant in the circumferential direction and the temperature is same.
- The heat flowing across the heater surface is divided into two quantities, heat entering the sheath beneath the fin and the heat entering the sheath between the fins.
- A temperature gradient exists in the circumferential direction since the sheath beneath the fin is cooler than the sheath between the fins due to fin effect. Therefore, The heat entering the sheath between fins flows into two directions, radially and circumferentially, due to temperature gradient.
- The heat entered into the sheath beneath the fin is convected away on the fin surface.

Under these assumptions, the heat balance for the 1/16 segment of the finned heater cross section shown in Fig. 1 can be expressed as,

$$\frac{Q_{fin}}{2} = Q_{sh} + q r_1 \phi_2 \tag{1}$$

The heat flow through the fin, Q_{fin} , and the circumferential heat transfer from the sheath to fin root region can be obtained by solving the steady state one dimensional heat conduction equation, respectively, below,

$$Q_{fin} = -kb \left.\frac{d\theta}{dx}\right|_{x=0} = kmb\,\theta_o \left[\frac{\frac{h_{ft}}{mk} + \tanh(mL)}{1 + \frac{h_{ft}}{mk}\tanh(mL)}\right] \tag{2}$$

where, $m = \sqrt{\frac{2h_{ft}}{kb}}$ and $\theta_{x=o} = \theta_o = T_o - T_b$

$$Q_{sh} = -tk\frac{1}{r_{av}} \left.\frac{d\phi}{d\phi}\right|_{\phi=\phi_1} = -tka\frac{1}{r_{av}}\left(\phi_o - \frac{r_1}{h_{sh} r_2}\, q\right)\tanh(a\,\phi_1) \tag{3}$$

where, $a = \sqrt{\frac{h_{sh}\, r_{av}\, r_2}{tk}}$ and $\phi = T(\phi) - T_t$

Substituting Eqs. (2) and (3) into Eq.(1) gives the temperature at the root of the fin as,

$$\theta_o = \frac{q}{h_{fs}} \frac{[a\, r_1 \phi_2 + r_1 \tanh(a\,\phi_1)]}{\left[a\, n \frac{2L + b\frac{h_{ft}}{h_{fs}}}{2} + \frac{r_2\, h_{sh}}{h_{fs}}\tanh(a\,\phi_1)\right]} \tag{4}$$

With the root temperature by Eq.(4), the heat flux distribution along the periphery of the finned geometry can be obtained from Eqs. (2) and (3) and the temperature distributions are calculated from the solutions of heat conduction equations, respectively.

This model can be used to calculate the heat flux distribution for the finned geometry at low flow CHF condition since the assumption of same boiling condition in both fin side and base between fins may be reasonable

to apply for the high quality CHF condition. Good agreement of the predictions was reported for the case of a finned geometry in the single phase condition where the heat transfer coefficients are expected to vary little along the periphery of surface [Kowalski et al.(1989)]. However, it should be noted that two dimensional approach is required to the CHF analysis with high subcooling and high velocity conditions due to the existence of a nonboiling region in the fin.

In order to analyze the obtained CHF data using the analytical model, a boiling heat transfer correlation is necessary because this estimation assumes the upper limit of boiling heat transfer as the CHF point in a boiling curve. In this study a modified Chen correlation, in which the convective component was substituted with the correlation determined for the finned geometry, was used to give the convective boundary conditions as below,

$$q = h_{1\phi}\,(T_w - T_b) + h_{2\phi}\,(T_w - T_{sat}) \tag{5}$$

where, $h_{1\phi} = 0.00214 \frac{k_b}{D_{hy}} Re_b^{1.033} \mathrm{Pr}_b^{0.615} \left(\frac{D_{hy}}{D_{he}}\right)^{0.154} F$

$$h_{2\phi} = 0.00122 \left[\frac{k_f^{0.79} C_{pf}^{0.45} \rho_f^{0.49}}{\sigma^{0.5} \mu_f^{0.29} h_{fg}^{0.24} \rho_g^{0.24}}\right] \Delta T_s^{0.24}\, \Delta P_s^{0.75} S$$

Iterations are needed to get the solution because the heat transfer correlation is a function of wall temperature. In the course of heat flux estimation, whether or not the wall temperature exceeded the ONB temperature was calculated by the following correlation, which was derived using the experimental data similar to the thermal hydraulic conditions of present study.

$$T_{w,onb} = T_s + \frac{8\sigma_s T_{s,K} v_{fg} h_{1\phi}}{h_{fg} k_s}\left[0.0305 Re_b^{-1.182} \mathrm{Pr}_b^{-3.171}\left(\frac{C_{pf}\Delta T}{h_{fg}}\right)^{1.631}\left(\frac{\rho_f}{\rho_g}\right)^{0.694}\right] \quad (6)$$

Fig. 2 shows the ratio of average heat transfer coefficient predicted by Eq.(1) to the measured one along with velocity which were evaluated using the actual heated surface area and the arithmetic mean of the measured fin tip and sheath temperatures. The figure indicates that the modified Chen correlation agrees well with the experimental data as the velocity decreases while some discrepancies occur at the high velocity conditions. Hence, Eq.(1) can be applied to determine the local heat flux distribution of low flow CHF along the periphery of the sheath including the fin. The typical result of the heat flux and the wall temperature predicted by the analytical model is depicted in Fig. 3. The predicted wall temperature at the sheath between the fins where the maximum heat flux is expected agrees well with the measured one, but shows some overprediction at the fin tip. The calculation by the two dimensional code of TEMP2D[Lim et al(1988)] also gives a similar result except for a slightly lower heat flux at the fin side. This may be caused by the use of a bulk temperature of fluid as boundary condition although the coolant temperature actually varies around the periphery of the fin. Fig. 4 depicts the ratio of the predicted to the measured wall temperature at the sheath between fins for the experimental data. Because it shows good agreements, the analytical model is used to estimate the local CHF for the finned geometry at low flow and low pressure conditions.

5. Results and Discussions

5.1 Parametric Trends

In investigating parametric trends two points of view can be represented .ie.; CHF as a consequence of local conditions and CHF as a consequence of system describing parameters. In this study, the major parametric trends of the experimental data were analyzed based on fixed inlet conditions from the latter viewpoint. This is because it is difficult to measure and to estimate the exact local parameters in low flow and low pressure conditions and the local condition hypothesis is not sufficient to describe the CHF in this region[Chang et al.(1991)]. It is noted that the effects of nonequilibrium voids and heat flux are particularly important at low pressures and low flow conditions, especially in the annulus geometry.

Mass flux effect

Fig. 5 depicts the parametric effect of mass flux on CHF. CHF increases with mass flux, but a different gradient of the curve is shown for larger mass fluxes of about 180 $kg/m^2/s$. This is very similar to the values reported by El-Genk et al.(1988) and Rogers et al.(1982). One reason for this may be supposed as; For relatively low flow rates, the increase of flow linearly increases CHF because CHF is caused by the liquid film depletion due mainly to the evaporation. However, the higher flow rate and heat flux will result in the increase of entrainment which leads to an early liquid film depletion or breakdown, and consequently a lower CHF.

Inlet subcooling effect

For a given mass flux, the CHF increases with increasing inlet

subcooling as shown in Fig. 6. It is believed that the increase of initial liquid film thickness owing to the shortened two phase length by high subcooling leads to higher CHF. It is noted that the subcooling effect does not clearly appear for lower mass flux since CHF occurs at high quality conditions as mass flux decreases, and the range of inlet subcooling, which can be actually controlled in the experiment at low pressure, is relatively smaller than the latent heat.

Pressure effect

As the system pressure is coupled with the fluid properties such as density and subcooling, it may be difficult to give the separate effect of pressure on the CHF. However, it can be presumed from Fig. 7 that the CHF increases slightly with the increase of pressure for a fixed mass flux and inlet subcooling conditions. This can be explained by the fact that the location of the onset of annular flow moves downstream as the pressure increases, and thicker initial liquid film results in a larger CHF.

Heated length effect

The CHF decreases as the heated length increases, as shown in Fig. 8. Thicker initial liquid film due to the shortened two phase length might result in higher CHF. However, the effect looks to be a little bit smaller as the mass flux decreases.

Hydraulic diameter effect

The CHF increases with the increase of the hydraulic diameter as shown in Fig 9. This behavior appears to be the results of a relatively lower quality in a larger channel, which means more participation of liquid in cooling heater surface and thicker liquid film due to the decrease of quality. Fig 10 indicates that the critical quality at CHF condition, which is

calculated by the steady state heat balance of Eq.(7) with the assumption of thermodynamic equilibrium, decreases as mass flux increases.

$$X_c = \frac{1}{h_{fg}}\left(\frac{A_h\, q_{chf}}{A_f\, G} - \Delta h_i\right) \tag{7}$$

It can be drawn from the figures that the unheated wall effect on the CHF increases as the mass flux and the hydraulic diameter increase.

5.2 *Fin effect on CHF*

At the same inlet conditions of mass flux and subcooling, the critical power ratio between the finned and the unfinned geometries is depicted in Fig 11. The critical power of finned geometry is higher than that of unfinned geometry by about 17% on average (12.7% for mass flux range smaller than 150 kg/m^2/s and 23.5% for larger than 150 kg/m^2/s) due to larger heat transfer area. The difference of flow area is only 4%. Here, it is interesting that the latter value of 23.5% is similar to 26% of difference between the two geometries' hydraulic diameters. The smaller ratios for the lower mass fluxes can be understood by the fact that the heat transferred to the coolant through the fins increases as mass flux decreases. In other words, the coolant enthalpy at lower flow reaches the condition for CHF occurrence more quickly than that for higher mass flux. Basically, the CHF is caused by the lack of cooling at the heater surface, and it depends on the fluid condition. Hence, it is necessary to compare the values of CHF at the same coolant condition. Fig. 12 shows that the comparison between the predicted CHF for finned geometry and the measured one for unfinned geometry at the same mass flux and the similar exit quality conditions. If we consider the hydraulic diameter effect on CHF with the assumption that $q_{chf} \sim D_{hy}^{-1/2}$ or $D_{he}^{-1/2}$[Groeneveld et al.

(1996)], the CHF for unfinned geometry should be 12.4% or 31.8% larger than that of the finned geometry. This tendency, however, cannot be found in this figure. Instead the two values are rather similar with each other. Hence, it may be drawn that the fin does not affect the CHF for low flow condition, although it increases the critical power due to larger heat transfer area.

5.3 *Comparison of Test Data with Existing Correlations*

The local CHF values at the sheath between the fins estimated by the analytical model were compared with the existing correlations for the prediction of CHF in an annulus with the unfinned geometry. The compared correlations are listed in table 3 with the applicable ranges.

Fig.s 13 ~ 20 show the results of comparisons between the experimental data and the existing CHF correlations. It can be seen that most of correlations give large deviations and scatters in predicting the experimental data for finned geometry. However, the two correlations of El-Genk et al.(1988) and Mishima et al.(1972) give reasonable predictions for the unfinned geometry. The figures also show that CHF values of the finned geometries are quite different from those of unfinned geometries for the same inlet flow rate, inlet subcooling and pressure conditions.

The Kowalski et al.(1994) correlation, which is applicable to the finned geometry in high flow rate and high subcooling conditions, shows a trend of overprediction as the mass flux decreases although the inclusion of fin effect appears to some extent. The AECL lookup table[Groeneveld et al.(1986)] for tube geometry overpredicts monotonically as the mass flux increases. It may be caused by the cold wall effect, that is, the smaller participation of liquid to cool heat surface for higher mass flux and larger

hydraulic diameter.

A remarkable point is that the two correlations of El-Genk et al.(1988) and Mishima et al.(1972) developed on the basis of the heat balance and the flow pattern transitions, give systematic deviations of CHF values for the finned and unfinned geometries. This implies that the CHF in an annulus at low flow conditions is dependent on the heat input to coolant and the flow pattern, especially annular flow. Fig 21 and 22 present the CHF data for finned and unfinned geometries at 110 kPa plotted on the two phase flow regime map based on the drift flux model[Mishima & Ishii(1984)]. These figures suggest most of the data fall on the annular flows. The inlet subcooling influence on the flow pattern is small. However, it is noted that the classification between the annular flow and annular mist flow is supposed to be qualitative because of the uncertainties of the flow regime map itself, and also because of the use of equilibrium exit quality. And it is not so important to derive a correlation from getting the correlation constants by fitting the data.

5.4 Development of CHF Correlation

As shown in the previous figures, the existing CHF correlations for annulus or tube geometries are not applicable for the finned geometry. Two correlations based on the heat balance give a suggestion for the development of CHF correlation. Hence, to develop a new CHF correlation for both finned and unfinned geometries, the following heat balance equation in a dimensionless form is used in this study.

$$q^*_{chf}\left(\frac{A_h}{A_f}\right) = \left[\sqrt{\frac{\rho_g}{\lambda g \Delta\rho}}\, j_g + \frac{\Delta h_i}{h_{fg}}\, G_*\right] \tag{8}$$

where, $q^* = q/(h_{fg}\sqrt{\lambda \rho_g g \Delta\rho})$

$$G^* = G/\sqrt{\lambda \rho_g g \Delta\rho}$$

$$\lambda = \sqrt{\sigma/g\Delta\rho}$$

The first term on the right hand side depends on the void fraction distribution and quality at CHF condition. However, it is quite difficult to estimate or measure this term at the annular flow in the annulus, especially under low flow and low pressure conditions. As well, the equation does not describe properly the parametric effects such as pressure and fin geometry as shown in Fig 15 and 16. The following relationship is, therefore, proposed to predict the CHF on the finned surface, including terms to describe these effects.

$$q''_{chf}\left(\frac{A_h}{A_f}\right) = C_1(L/D_{he})^{C_2}\left(C_3 + C_4\frac{\Delta h_i}{h_{fg}}G^*\right)\left(\frac{\rho_f}{\rho_g}\right)^{C_5}\left(\frac{P_h}{P_r}\right)^{C_6} We^{C_7} \qquad (9)$$

The coefficients of Eq.(9) were obtained by the regression of the experimental CHF data as ; $C_1 = 0.3$, $C_2 = 0.29$, $C_3 = 2.67$, $C_4 = 0.08$, $C_5 = 0.1$, $C_6 = 1.07$, $C_7 = 0.23$

Fig 23 presents the comparison of Eq.(9) with the CHF data for both finned and unfinned geometries. Reasonable predictions are shown with an RMS error of 13.7% and mean (M/P) of 1.001. The parametric trends are correctly predicted by the proposed correlation. Hence, the suggested correlation of Eq.(9) is valid for the finned and unfinned geometries in the ranges given in table 2.

6. Conclusion

Experiment and analysis were performed in a vertical annulus with both finned and unfinned geometries at the low flow and low pressure conditions. The parametric trends for the obtained data were examined

together with the fin effect on CHF and the existing CHF correlations were compared with the experimental data. A new CHF correlation was proposed to predict the CHF for both finned and unfinned geometries.

The conclusions of the present work are as follows:

(1) The parametric trends of the CHF data for the finned geometry agreed with the general understandings from the previous studies for the unfinned annulus or tube geometries. That is, CHF increases as the mass flux, inlet subcooling, pressure and hydraulic diameter increase and the heated length decreases.

(2) At the same inlet condition of mass flux and subcooling, the critical power for the finned geometry is higher than that for the unfinned geometry by about 17% of average due to larger heat transfer area. However, in view of local condition, the fin does not affect CHF under low flow and low pressure conditions since the predicted CHF for the finned geometry is similar to that for the unfinned geometry at the same mass flux and the exit quality conditions.

(3) An analytical model with a modified Chen correlation was shown to be applied for estimating the distributions of the heat flux and the wall temperature for the finned geometry at the low flow CHF condition. The predicted maximum wall temperature at sheath midway between fins, where the maximum heat flux occurs, agreed well with the measured temperature, but a little overprediction at the fin tip was shown. This may be caused from the use of bulk fluid temperature as boundary condition although the coolant temperature actually varies around the periphery of the fin.

(4) A new correlation is proposed as Eq.(9) to predict the CHF for both finned and unfinned geometries at low flow and low pressure conditions. The predictions by the developed correlation show reasonable agreements with the experimental data. An RMS error was 13.7 %.

Nomenclature

A_f	Flow area of a channel	A_h	Heated area of a channel
C_{pf}	Specific heat	D	Tube diameter
D_{he}	Heated equivalent diameter	D_{hy}	Hydraulic equivalent dia.
G	Mass flux	g	Gravitational acceleration
h	Heat transfer coefficient	h_{fg}	Latent heat of vaporization
Δh_i	Inlet subcooling or Local enthalpy	k	Conductivity
L	Length of a heated channel	q_{chf}	Critical heat flux
Q_{fin}	Heat flow through the fin	Q_{sh}	Circumferential heat transfer from sheath to fin root
P_h	Actual perimeter of heater	P_r	Perimeter based on base dia. of heater
Pr	Prandtl number	Re	Reynolds number
r_1, r_2	Inner and outer radius of sheath	s	Gap thickness of annulus
t	Thickness of the aluminium sheath	T	Temperature
v	Specific volume	w	Width of Fin
We	Weber number		

Greek Symbols

ρ	Density	σ	Surface tension
$\Delta\rho$	Liquid-vapor density difference	μ	Dynamic viscosity
ϕ	Azimuthal angle	1ϕ, 2ϕ	Single and Two Phase

Subscripts

av	Average	b	Bulk fluid
fs	Side of fin	ft	Tip of fin
i	Inner or Inlet	f	Liquid
g	Vapor	s	Saturation
fg	Difference between saturated vapor and liquid		
sh	Sheath	w	Wall
o	Root of fin		

Superscripts

*	Nondimensional variables

References

Araki, M. et al., "Burnout Experiments on the Experimentally Finned Swirl Tube for Steady-State High Heat Flux Beam Stops," Fusion Eng. Des., 9, (1989) 231-236

Bennet, A.W. et al.,"Studies of Burnout in Boiling Heat Transfer," Trans. Instn. Chem. Eng., 45, (1967) 319-339

Chang,S.H., Baek,W.P. Bae,T.M.,"A Study of CHF for Low Flow of Water in Vertical Round Tubes under Low Pressure," Nucl. Eng. Des., 132, (1991)

Collier,J.G., Convective Boiling and Condensation, Mcgraw-Hill, 1972.

El-Genk, M.S. et al.,"Experimental Studies of Critical Heat Flux for Low Flow of Water in Vertical Annuli at Near Atmospheric Pressure," Int. J. of Heat Mass Transfer, 31, (1988) .2291-2304

Grimley, T.A. et al., "CHF Enhancement in Flowing Fluorocarbon Liquid Films using Structured Surfaces and Flow Deflectors," Int. J. of Heat Mass Transfer, 31., (1988) 55-65

Groeneveld, D.C.,et al., "1986 AECL-UO Critical Heat Flux Lookup Table," Heat Transfer Eng., 7, (1986) 46-62

Groeneveld, D.C., et al., "The 1995 Look-up Table for Critical Heat Flux in Tubes," Nucl. Eng. Des., 163, (1996) 1-23

HANARO Safety Analysis Report, KAERI, KAERI/TR-710/96, June, 1996.

Katto, Y., " A Generalized Correlation of CHF for Forced Convection Boiling in Vertical Uniformly Heated Round Tubes," Int. J. Heat Mass Transfer 21, (1978),1527-1542

Kowalski, J.E. et al, "Heat Flux Distribution on a Finned Fuel Pin," 15th Annual Nuclear Simulation Symposium, Missiauga, Canada, (1989)

Kowalski, J.E. et al.,"Analysis of Critical Heat Flux during Subcooled Boiling for Finned Fuel Elements," Nucl. Eng. Des., 149, (1994) 177-184

Lim,I.C. et al., "Development of a 2D Conduction Code for KMRR Fuel element Analysis," 3rd Int. Topical Meeting on Nuclear Power Plant T/H and Operations, Seoul, (1988)

Meyer, G., et al., "Comparision between the Critical heat Fluxes for a Finned Tube and for a Plane Tube in a Cross Flow," Proc. 5th Int. Symp. on Multi-phase Heat Transport and Particulate Phenomena, (1988)

Mishima, K. and Ishii,M., "Flow Regime Transition Criteria for Upward Two phase Flow in Vertical Tubes," Int. J. of Heat mass Transfer .27, (1984) 723-737.

Mishima, K. and Ishii,M., CHF Experiments under Low-flow Conditions in a Vertical Annulus, NUREG/CR-2647, 1982

Park, C. et al., HANARO Single Element Critical Heat Flux Experiment under Low Flow Condition, KAERI/TR-880/97, 1997

Rogers et al., "Flow Boiling CHFs for Water in a Vertical Annulus at Low Pressure and Velocities," Proc. 7th Int. Heat Transfer Conf., 4, (1982) FB28

Shim, S.Y. et al.,"Critical Heat Flux in Subcooled Flow Boiling on Finned and Unfinned Tube Geometries," Proceedings of AIAA/ASME Thermalpyhysics and Heat Transfer Conf., 138., (1990) 91-98

Table 1. Test Section Geometries

Type of FES	Length (m)	Quartz Tube I.D.(mm)	Hydraulic Dia.(mm)	# of Data
Finned	0.7	17	7.3	74
Finned	0.7	24	13.66	15
Finned	0.6	17	7.3	10
Unfinned	0.7	17	9.2	48

Table 2. Experimental Range of Data

Parameter	Range	Uncertainty
Pressure(kPa)	110～509	± 1%
Mass Flux(kg/m^2/s)	26～404	± 3%
Inlet Subcooling(kJ/kg)	176～500	± 1%
Heat Flux (kW/m^2)	258～1415	± 4%
Critical Quality	-0.034～0.702	

Table 3. Annulus CHF Correlations

Correlations	Applicable Range
■ **Barnett(1966)** $q_{chf} = \frac{A(h_{fg}/649) + B\,\Delta h_i}{C + L_h}$ where, $A = 67.45 D_{hy}^{0.68} (G*10^{-6})^{0.192} [1 - 0.744 \exp(-6.512 D_{he} (G*10^{-6}))]$ $B = 0.2587 D_{hy}^{1.261} (G*10^{-6})^{0.817}$ $C = 185.0 D_{he}^{1.415} (G*10^{-6})^{0.212}$	- P ; 415 ~ 965 kPa - G ; 190 ~8430 kg/m^2/s - L_h ; 0.61 ~ 2.74 m - D_i ; 9.5 ~ 96.5 mm - D_o ; 14 ~ 101.6 mm - L_h , D_{he} ; inch - q_{chf} ;Btu/hr/ft^2 * 10^{-6} - 0 < Δh_i < 958 kJ/kg
■ **Knoebel(1973)** $q_{chf} = 1360 (\frac{We}{Re})^{0.573} (\rho C_p T_i)^{0.759} (\rho C_p)^{0.621} k^{0.19}$ where, $We = \frac{G^2 D_{hy}}{\sigma \rho_f}$, $Re = \frac{G D_{hy}}{\mu_f}$, $T_i = T_{sat} - T_b$	- P ; 30 ~ 95 Psia - V ; 15 ~ 60 ft/s - L_h ; 0.5 m - V ; ft/s, T; °F - Cp; Btu/lbm/ °F
■ **Katto(1979)** $q_{chf} = q_{co} (1 + K \frac{\Delta h_i}{h_{fg}})$ **for L-regime,** $q_{co} = 0.25 G h_{fg} (\frac{\sigma \rho_f}{G^2 L_h})^{0.043} (D_{he}/L_h)$, $K = 1.0$ **for H-regime,** $q_{co} = 0.12 G h_{fg} (\frac{\rho_g}{\rho_f})^{0.133} (\frac{\sigma \rho_f}{G^2 L_h})^{1/3} (\frac{1}{1 + 0.0081 L_h/D_{he}})$ $K = 0.057 (69.2 D_{he}/L_h)^{11.0(\frac{\rho_g}{\rho_f})} (\frac{\sigma \rho_f}{G^2 L_h})^{-1/3}$	- h ; kJ/kg - G ; kg/m^2/s - L_h ; 0.48 m - D_{he} ; m - σ ; N/m - ρ ; kg/m^3
■ **Mishima(1982)** **for churn to annular flow,** $q_{chf} = \frac{A_f}{A_h} [G \Delta h_i + (\frac{1}{C_0} - 0.11) h_{fg} (\rho_g g \Delta\rho D_{hy})^{1/2}]$	- P ; 103 kPa - G ; 0 ~ 40 kg/m^2/s - L_h ; 0.6 m - D_{hy} ; 5.51 mm - D_{he} ; 12.5 mm

Table 3. Annulus CHF Correlations (Continued)

Correlations	Applicable Range
■ **El-genk(1988)** **for slug-churn/churn-annular flow,** $q^*(\frac{A_h}{A_f}) = 1.65(\frac{L_h}{D_{he}})^{0.2}[0.933+0.212G^*\frac{\Delta h_i}{h_{fg}}]$ **for annular to annular mist flow,** $q^*(\frac{A_h}{A_f}) = 0.85+1.045G^*\frac{\Delta h_i}{h_{fg}}]$ where, $q^* = Q/(h_{fg}A_h\sqrt{\lambda g\rho_g\Delta\rho})$, $G^* = G/\sqrt{\lambda g\rho_g\Delta\rho}$ $\lambda = \sqrt{\sigma/g\Delta\rho}$	- P ; 118 kPa - G ; 0 ~ 260 kg/m^2/s - L_h ; 0.5 m - D_{hy} ; 7.3 ~ 12.7 mm - D_{he} ; 18.8 ~ 38.1 mm - D_i ; 13 mm - D_o ; 20 ~25 mm
■ **Kumamaru(1990)** $\frac{q_{chf}}{G\,h_{fg}} = \frac{a}{(l_{bo}/D_{he})^b}$ where, a=0.0045, b=0.33 for $l_{bo}/D_{he} < 300$, a=0.081, b=0.84 for $300 < l_{bo}/D_{he} < 1000$, a=0.25, b=1.0 for $l_{bo}/D_{he} > 1000$	- P ; 3000 kPa - G ; 105 ~ 320 kg/m^2/s - Xe; 0.15 ~ 0.9
■ **Kowalski(1994)** $\frac{q_{CHF}}{q_{PB}} = 1+1.9472X10^{-4}(\frac{G^2D_{hy}}{\sigma\,\rho_f})^{0.633}(\frac{\rho_L}{\rho_g})^{0.584}(\frac{D_{hy}}{D_r})^{0.222}(\frac{P_{he}}{P_d})^{0.976}$ where, $q_{PB} = 0.273h_{fg}\rho_g U_B(1+Ja_m)^{0.87}(\rho_g/\rho_L)^{0.1}$ $Ja_m = -0.1x_{eq}(\rho_L/\rho_g)^{0.75}$, for $x_{eq}<0$ $Ja_m = -x_{eq}$, for $x_{eq}>0$ $U_B = [\sigma_g(\frac{\rho_L-\rho_g}{\rho_g^2})]^{0.25}$	- P ; 110 ~ 335 kPa - G ; 390 ~8405 kg/m^2/s - Xe ; -0.162 ~ 0.073 - q_{chf} ;0.89~11.2 MW/m^2 - $0.89 < D_{hy}/D_r < 1.76$ - $0.91 < P_{he}/P_a < 1.34$ - P_d = 41.2 mm

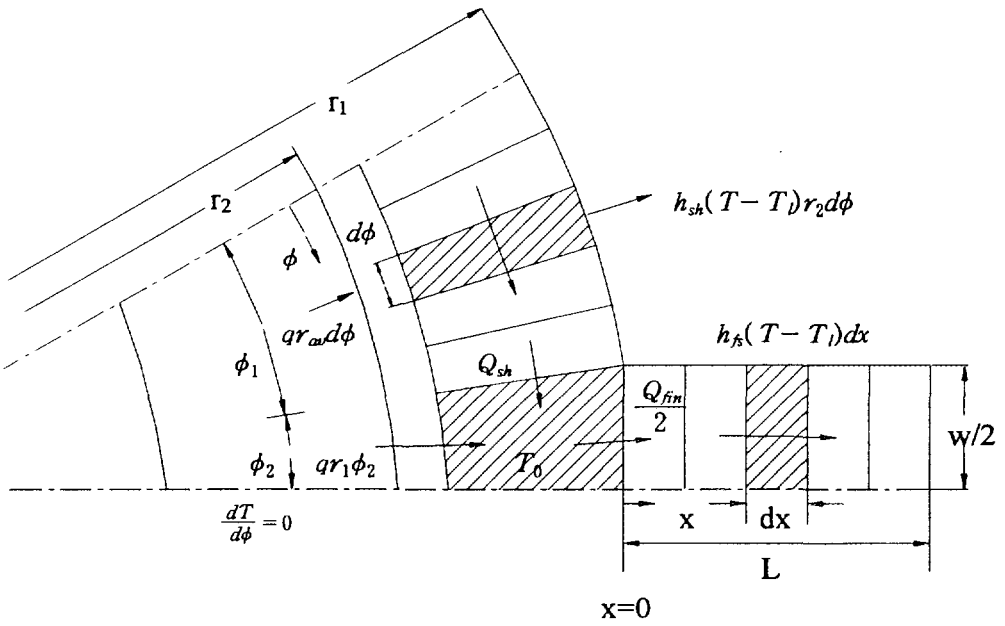

Fig. 1 Analytical Model for the Calculation of Heat Flux and Temperature Distribution

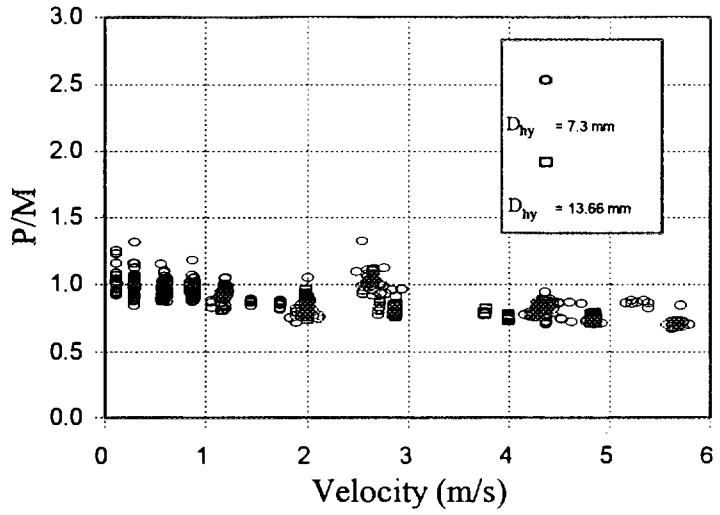

Fig. 2 Predicted to Measured Average Heat Transfer Coefficient Ratio

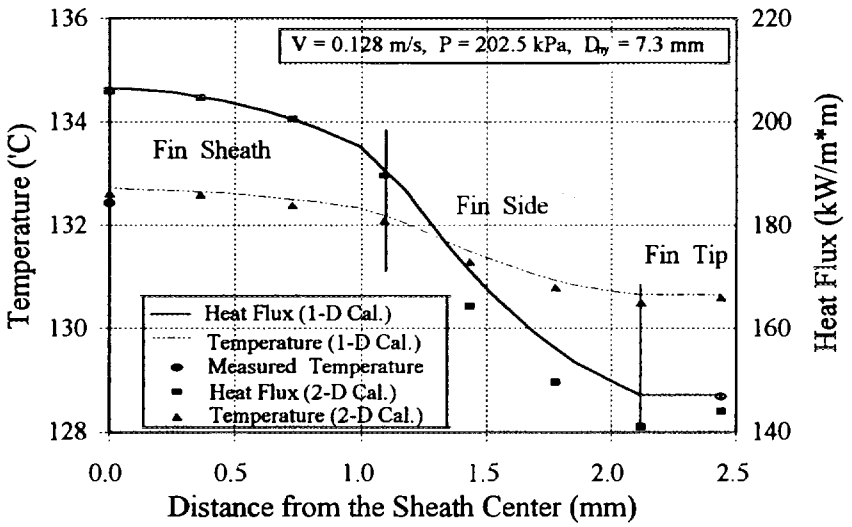

Fig. 3 Predicted Distribution of Heat Flux and Temperature around the Periphery of Finned Heater

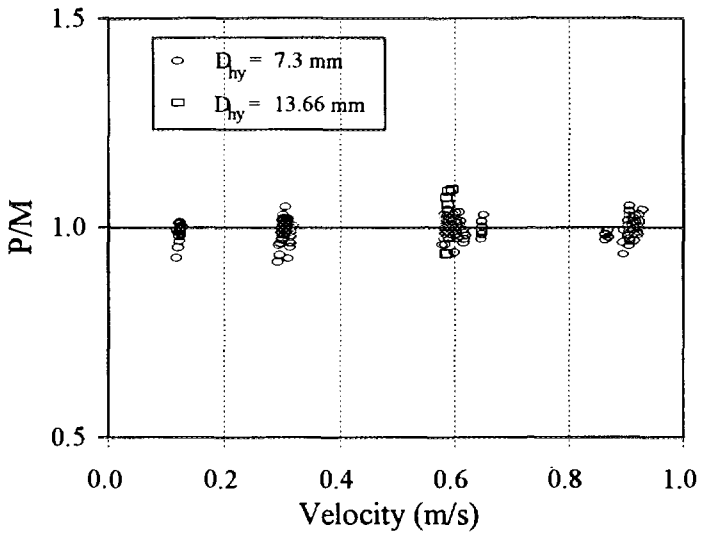

Fig. 4 Predicted to Measured Maximum Wall Temperature Ratio

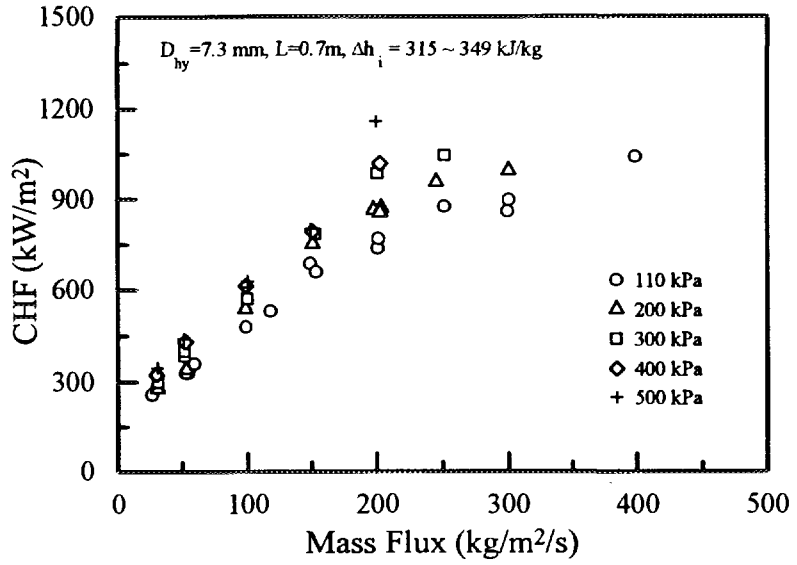

Fig. 5 Mass Flux Effect on CHF for a Finned Geometry

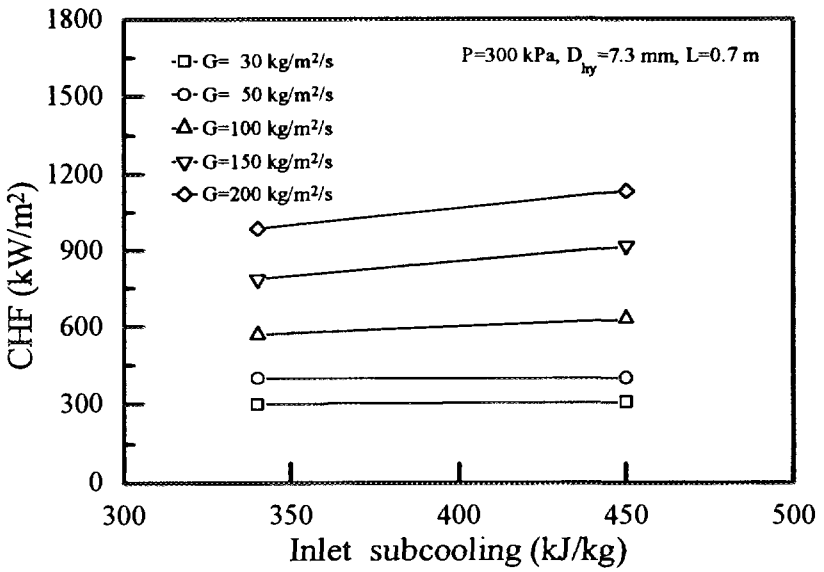

Fig. 6 Inlet Subcooling Effect on CHF for a Finned Geometry

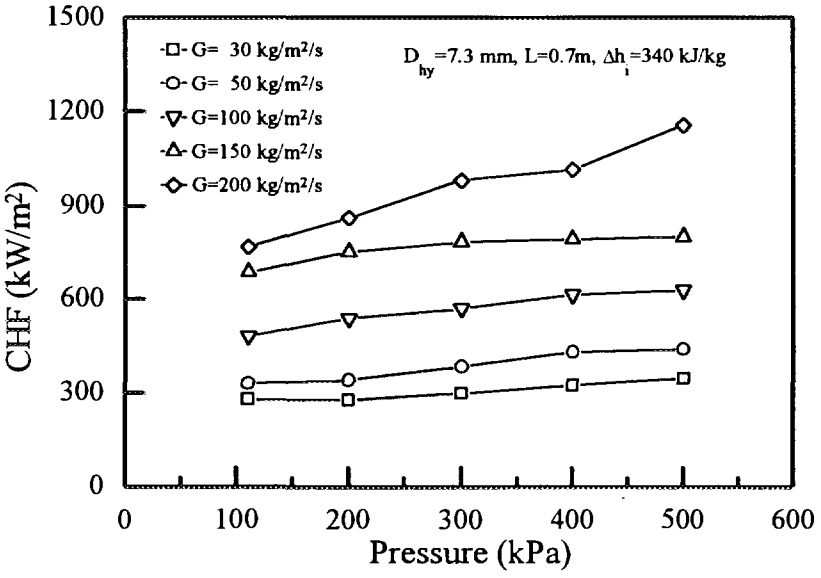

Fig. 7 Pressure Effect on CHF for a Finned Geometry

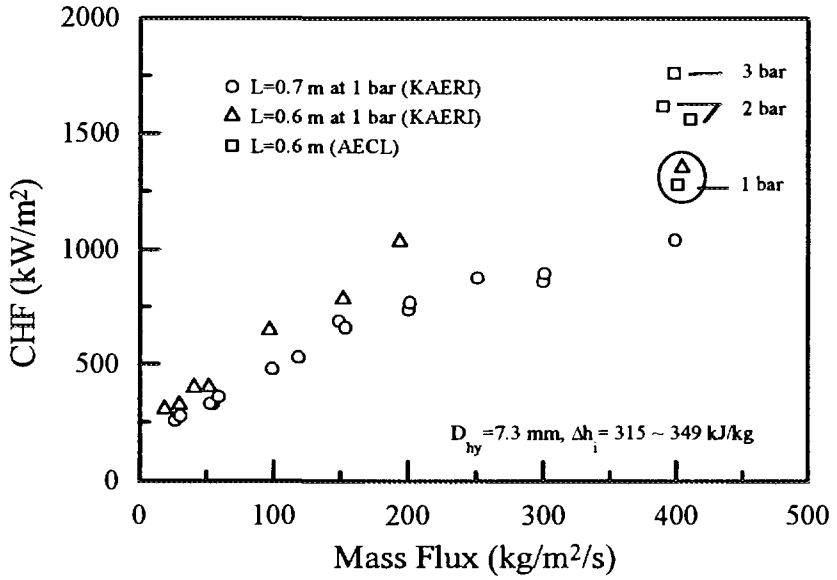

Fig. 8 Heated Length Effect on CHF for a Finned Geometry

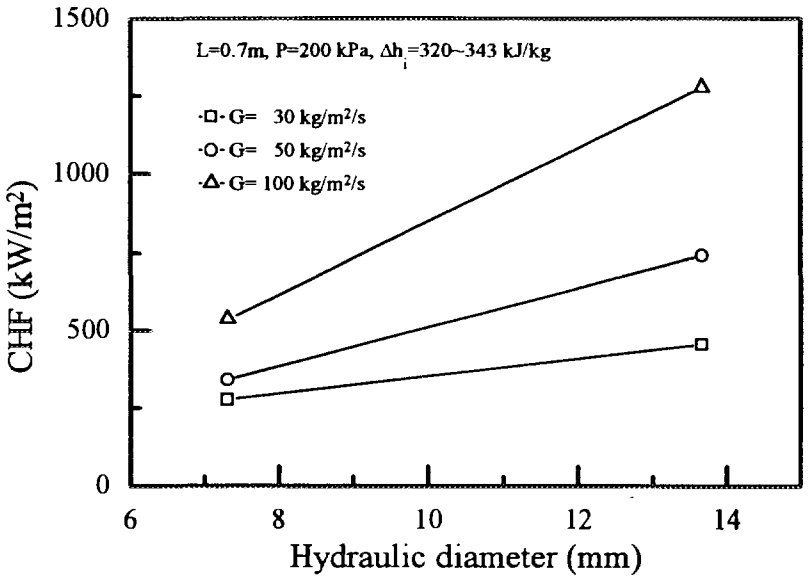

Fig. 9 Hydraulic Diameter Effect on CHF for a Finned Geometry

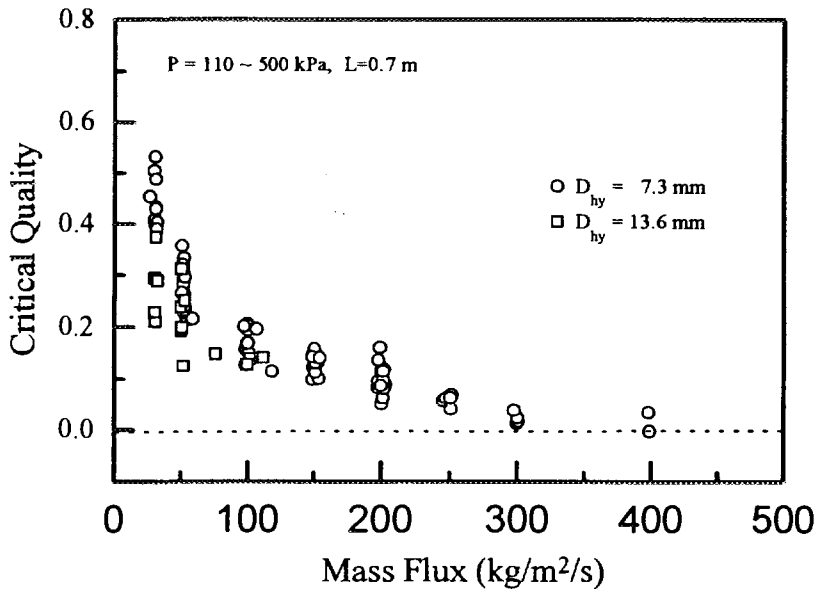

Fig. 10 Critical Quality at CHF Condition for a Finned Geometry

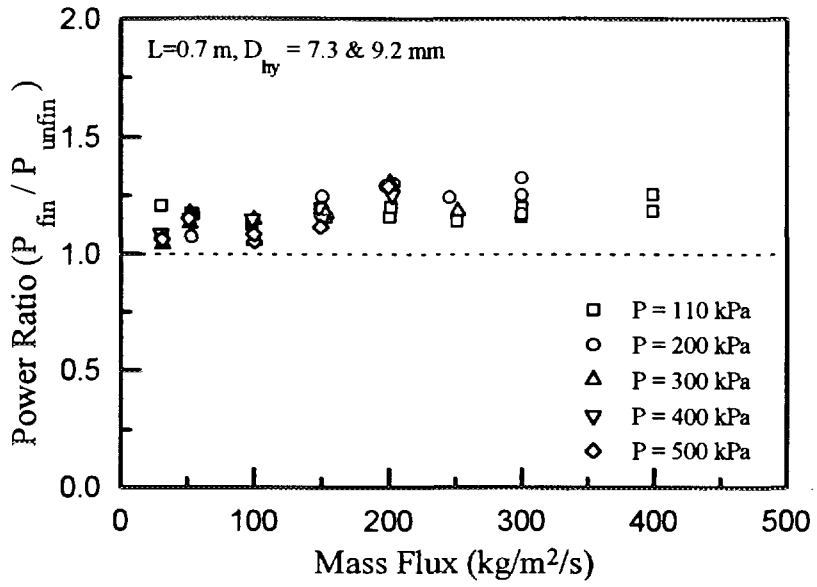

Fig. 11 Critical Power Ratios between Finned and Unfinned Geometries

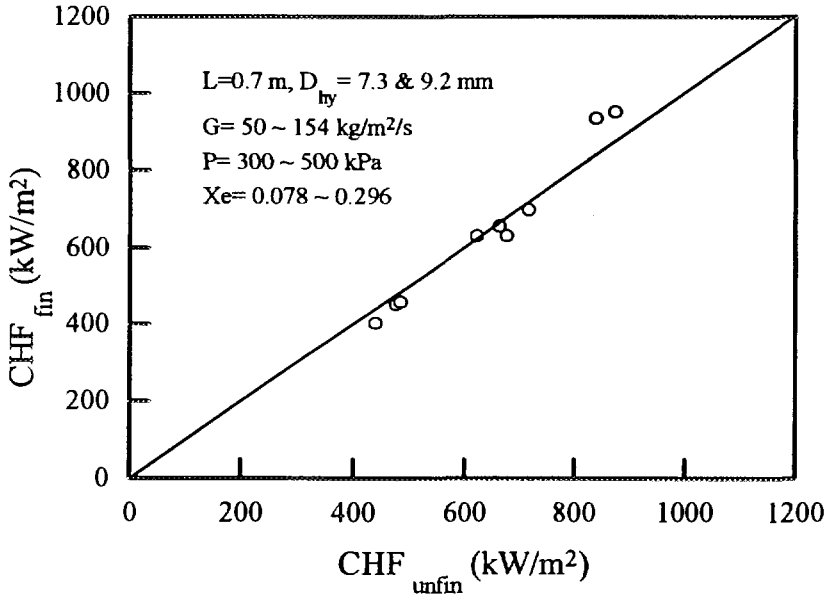

Fig. 12 Comparison of CHF values for the Finned and Unfinned Geometries at the Same Exit Coolant Conditions

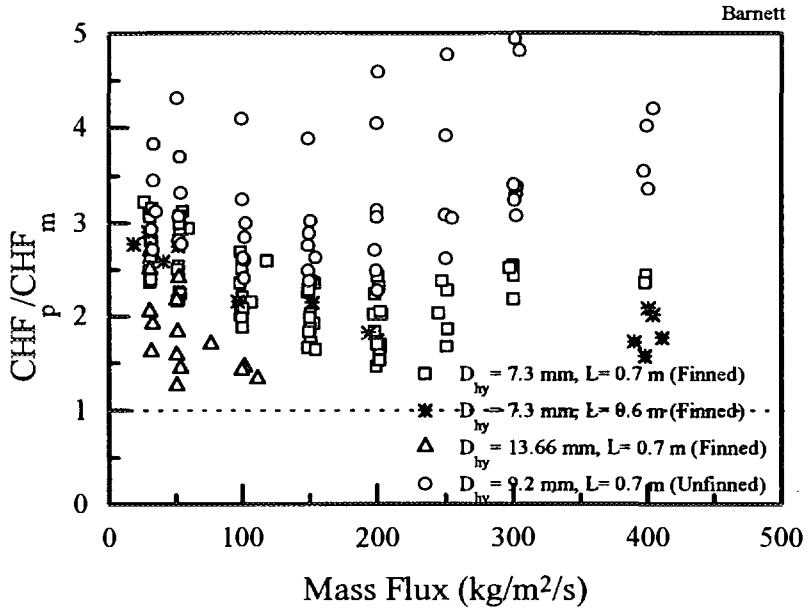

Fig. 13 Prediction of CHF Data by Barnett Correlation

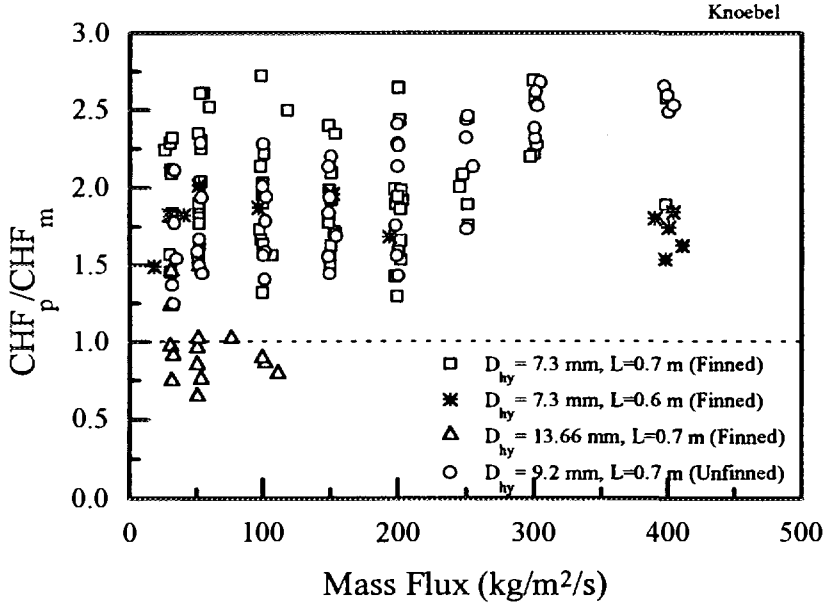

Fig. 14 Prediction of CHF Data by Knoebel Correlation

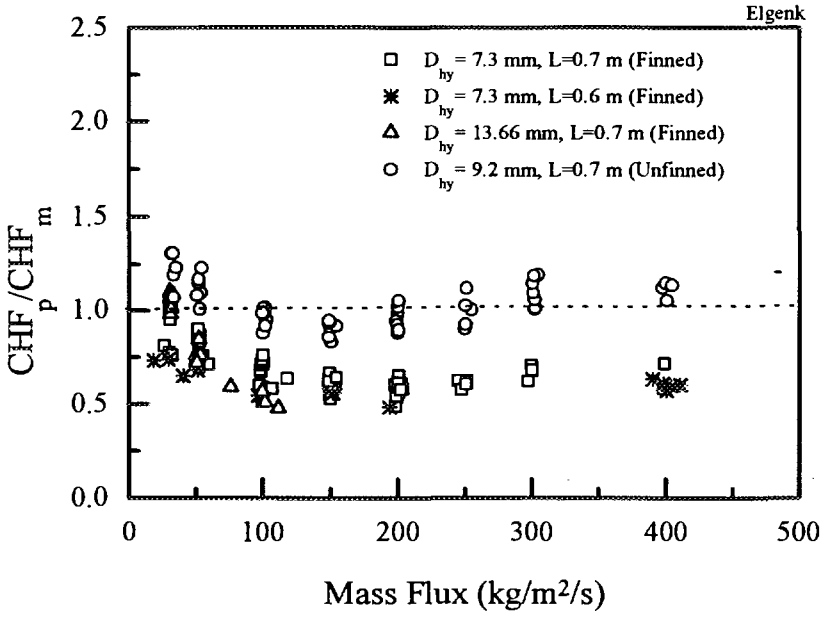

Fig. 15 Prediction of CHF Data by El-genk Correlation

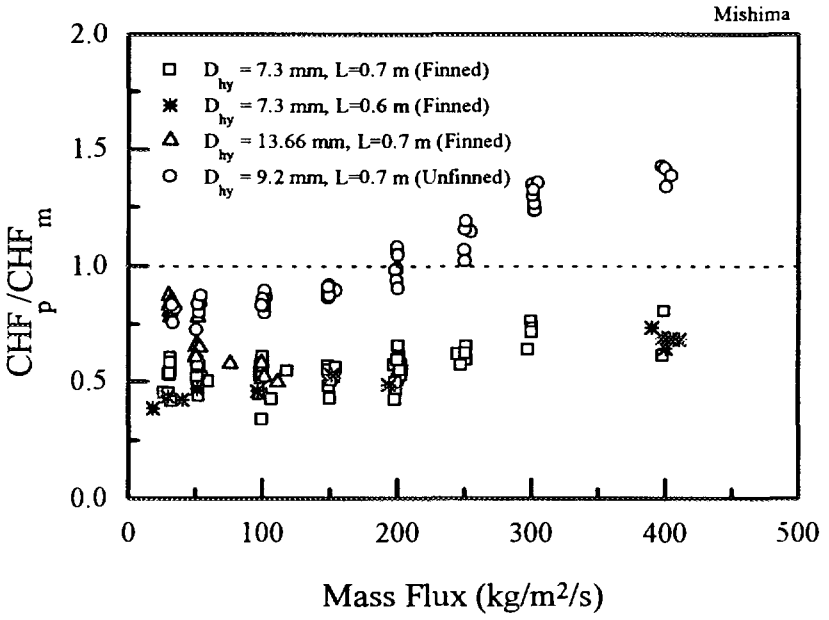

Fig. 16 Prediction of CHF Data by Mishima Correlation

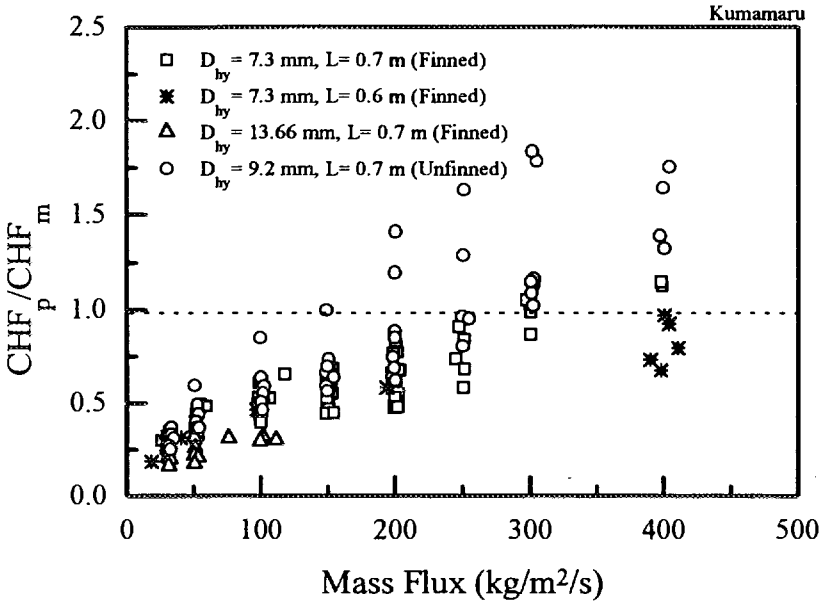

Fig. 17 Prediction of CHF Data by Kumamaru Correlation

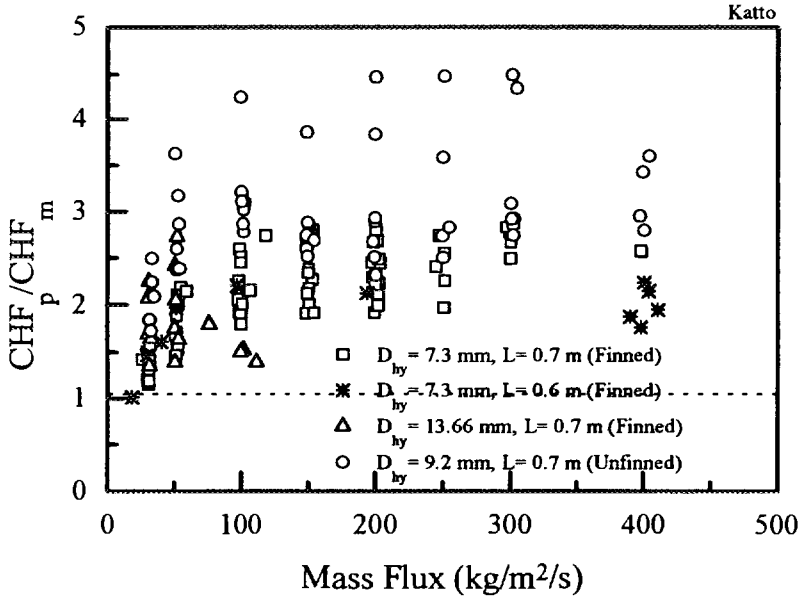

Fig. 18 Prediction of CHF Data by Katto Correlation

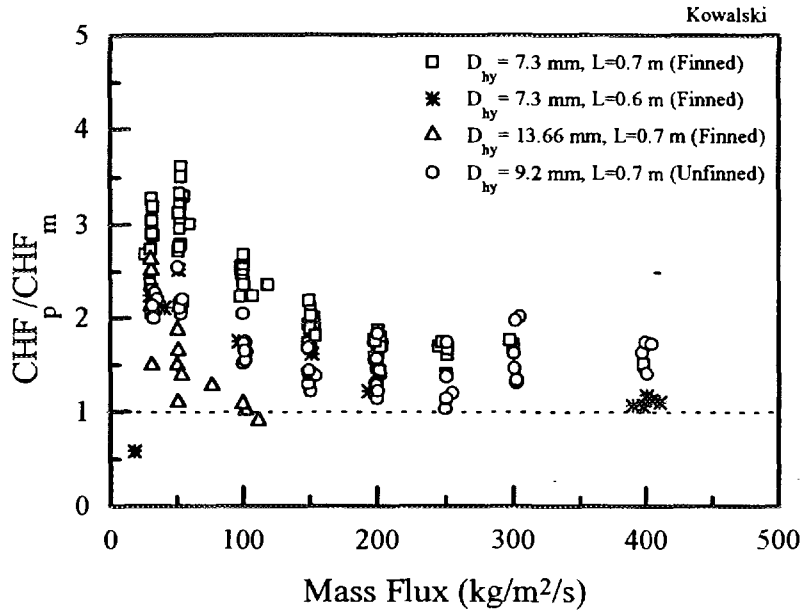

Fig. 19 Prediction of CHF Data by Kowalski Correlation

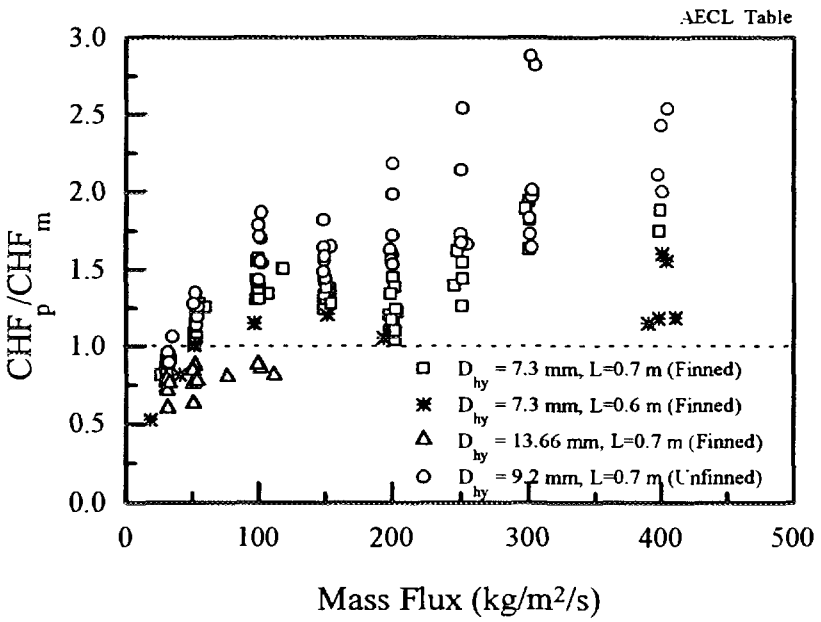

Fig. 20 Prediction of CHF Data by AECL Table

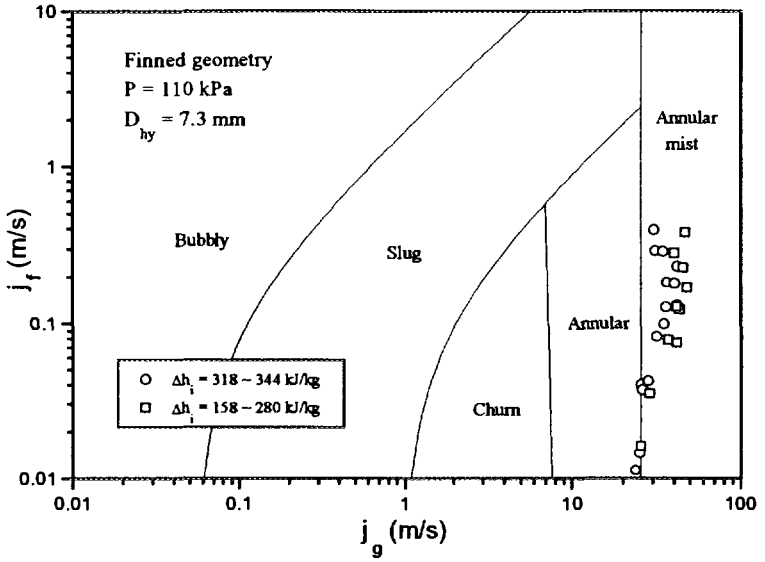

Fig. 21 CHF Data for the Finned Geometry Plotted on the Flow Regime Map

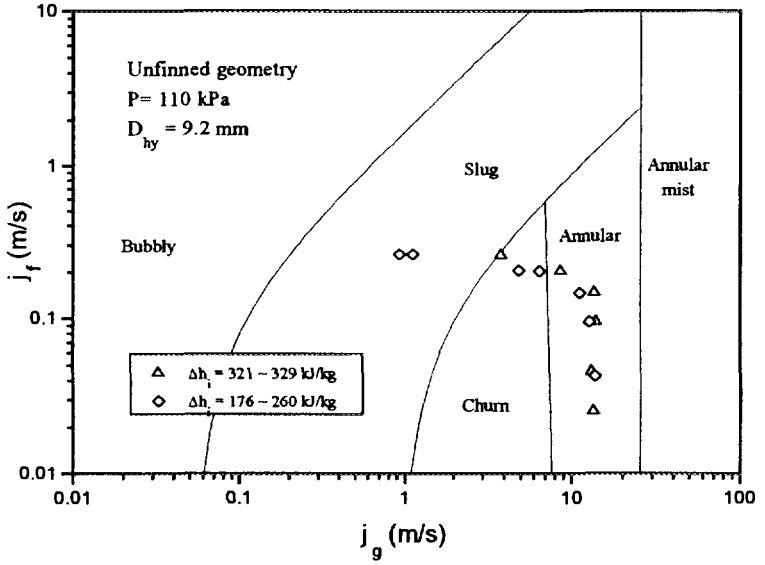

Fig. 22 CHF Data for the Unfinned Geometry Plotted on the Flow Regime Map

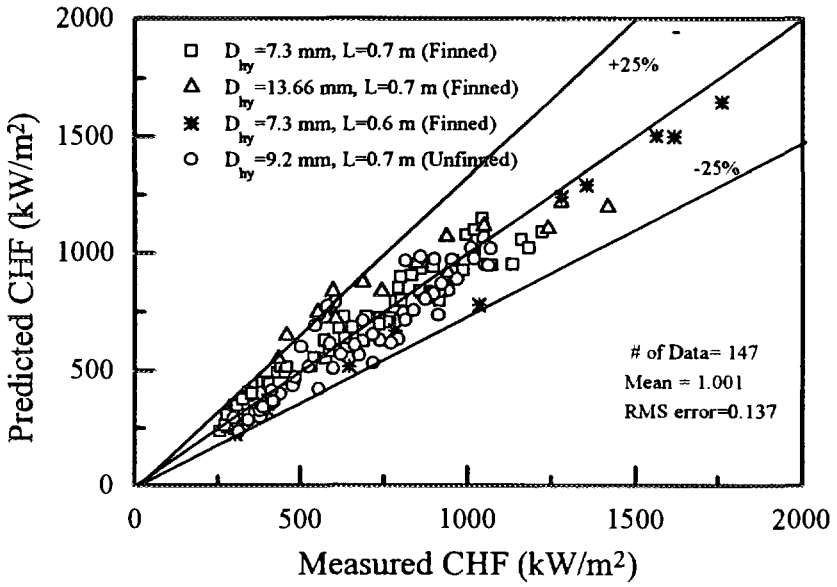

Fig. 23 Comparison of CHF Data with the Predictions by the Proposed Correlation

서 지 정 보 양 식

수행기관보고서번호	위탁기관보고서번호	표준보고서번호	INIS 주제 코드
KAERI/TR- /97			

제목/부제	하나로 저유속 임계열유속 상관식 개발
연구책임자 및 부서명 (AR 또는 TR인 경우:.주저자)	박 철, 하나로 운영팀
연구자 및 부서명	채희택, 한기양 (하나로 운영팀)

출판지	대 전	발행기관	한국원자력연구소	발행년	1997. 8.
페이지	36 p.	도 표	있음(O), 없음( )	크 기	29 x 21 Cm.
참고 사항					

비밀 여부	공개(O), 대외비( ), ___ 비밀	보고서 종류	기술보고서
연구위탁기관		계약 번호	

요약 (15-20 줄내외)

하나로의 자연대류 냉각 운전시 및 시고시 저유속 조건에서의 안전성 평가를 위한 임계열유속 상관식이 개발되었다. 임계열유속 조건에서 판이 있는 가열봉에 대해 둘레를 따른 온도 및 열유속 분포를 계산하기 위하여 해석적 모델을 사용하였으며, 모델에 의해 예측된 가열표면 온도와 측정된 온도는 잘 맞는 것으로 나타났다. 판이 달린 가열봉에서의 여러가지 변수가 임계열유속에 미치는 영향은 일반적으로 판이 없는 경우에 대해 알려진 경향과 일치하였다. 그리고, 판에 의한 열전달 면적의 차이로 인해 임계 출력은 증가하나 임계열유속은 차이가 없는 것으로 나타나 국부적으로 판은 임계열유속에 영향을 미치지 않는 것으로 판단된다. 기존의 판이 없는 경우에 대한 임계열유속 상관식들은 판이 있는 경우의 예측에서 큰 오차가 있는 것으로 나타나, 이를 보정한 새로운 상관식을 제시하였다. 새 상관식은 실험자료를 13.7%의 RMS 오차를 가지고 잘 예측한다. 상관식의 적용 범위는 아래와 같다.

- Pressure(kPa) 110 ~ 509 , - Mass Flux(kg/m^2/s) 26 ~ 404
- Inlet Subcooling(kJ/kg) 176 ~ 500 , - Heat Flux (kW/m^2) 258 ~ 1415
- Hydraulic Dia.(mm) 7.3 ~ 13.66, - Critical Quality -0.034 ~ 0.702

주제명 키워드 (10 단어 내외)	하나로, 임계열유속 상관식, 판

BIBLIOGRAPHIC INFORMATION SHEET

Performing Org. Report No.	Sponsoring Org. Report No.	Stamdard Report No.	INIS Subject Code
KAERI/TR- /97			

Title/ Subtitle	Development of Low Flow Critical Heat Flux Correlation for HANARO
Principal Author for AR/TR	Cheol Park, HANARO Operating Division
Researcher and Department	Hee-Taek Chae, Gee-Yang Han (HANARO Operating Division)

Publication Place	Taejon	Publisher	KAERI	Publication Date	1997. 7.
Page	36 p.	Ill. & Tab.	Yes(O), No ( )	Size	29 x 21 Cm.
Note					

Classified	Open(0), Restricted( ), ___ Class Document	Report Type	Technical Report
Sponsoring Org.		Contract No.	

Abstract (15-20 Lines)

A low flow CHF Correlation was developed for the safe operation of HANARO during the natural circulation cooling and the assessment of safety during the low flow condition of accident. The analytical model was applied to estimate the heat flux and the temperature distributions along the periphery of the fin at CHF conditions, and the predicted wall temperature at the sheath between the fins by the model agreeed well with the measured one. The parametric trends of the CHF data for the finned geometry agreed with the general understanding from the previous studies for the unfinned annulus or tube geometries. It is revealed that the fin does not affect the CHF for low flow condition, although it increases the critical power due to larger heat transfer area. As the existing CHF correlation for unfinned geometry gave large deviation in predicting the experimental CHF data, a new correlation is proposed to predict the CHF for both finned and unfinned geometries at low flow and low pressure conditions. The developed correlation predicts the experimental CHF data with RMS error of 13.7% The appricable range of CHF correlation is as follows,

- Pressure(kPa) 110 ~ 509 , - Mass Flux(kg/m^2/s) 26 ~ 404
- Inlet Subcooling(kJ/kg) 176 ~ 500 , - Heat Flux (kW/m^2) 258 ~ 1415
- Hydraulic Dia.(mm) 7.3 ~ 13.66, - Critical Quality -0.034 ~ 0.702

Subject Keywords (About 10 words)	HANARO, CHF Correlation, Fin